

Received July 19, 2019, accepted September 2, 2019, date of publication September 13, 2019,  
date of current version September 26, 2019.

Digital Object Identifier 10.1109/ACCESS.2019.2941399

# Fuzzy Adaptive-Equivalent Consumption Minimization Strategy for a Parallel Hybrid Electric Vehicle

SHUHAN WANG<sup>1,2</sup>, XINGSHUAI HUANG<sup>1,2</sup>, JOSÉ MARÍA LÓPEZ<sup>3</sup>,  
XIANGYANG XU<sup>1,2</sup>, AND PENG DONG<sup>1,2</sup>

<sup>1</sup>Department of Automotive Engineering, School of Transportation Science and Engineering, Beihang University, Beijing 100191, China

<sup>2</sup>Ningbo Institute of Technology (NIT), Beihang University, Ningbo 315323, China

<sup>3</sup>University Institute for Automobile Research (INSIA), Universidad Politécnica de Madrid, 28031 Madrid, Spain

Corresponding author: Peng Dong (dongpengbeihang@163.com)

This work was supported by the National Key Research and Development Program of China, Development and Vehicle Integration of Cost-Effective Commercial Vehicle Hybrid System, under Grant 2018YFB0105900.

**ABSTRACT** Hybrid electric vehicles (HEVs) have proved a feasible option to reduce fuel consumption and emissions. Furthermore, energy management strategies (EMSs) play a pivotal role in the performance of HEVs. This paper presents a novel real-time EMS, namely fuzzy adaptive-equivalent consumption minimization strategy (Fuzzy A-ECMS), for a parallel HEV. The proposed EMS is formulated by combining the ECMS, which is derived from Pontryagin's minimum principle (PMP), with a fuzzy logic controller adjusting the equivalent factor (EF) based on the deviation between reference state of charge (SOC) and actual SOC for a better SOC trajectory. Improved fuel economy and SOC charge sustainability are the main control objectives. To test and verify the performance of the studied controller, comparative simulations of the Fuzzy A-ECMS and rule-based EMS, conventional SOC-based A-ECMS together with standard ECMS under different standard driving cycles and a real driving cycle are conducted via MATLAB/Simulink and AVL CRUISE. The simulation results show the feasibility and effectiveness of Fuzzy A-ECMS, yielding 0.46% to 5.91% reduction of fuel consumption and more stable SOC charge sustainability compared with the other three EMSs.

**INDEX TERMS** Hybrid electric vehicle (HEV), energy management strategy (EMS), equivalent consumption minimization strategy (ECMS), fuzzy logic control, state of charge (SOC).

## I. INTRODUCTION

The gradual decline in global crude oil sources and stringent emissions rules have caused the urgent demand for vehicles with better fuel economy along with less emissions [1]. HEVs are widely considered as one of the most promising solutions to achieve the goals for their high efficiency and low fuel consumption. The powertrain system of HEV generally contains two different types of components, internal combustion engine (ICE) and electric motor (EM), which makes it operate more efficiently and effectively. EMSs are of great significance as they determine the power split ratio between two different power sources, engine and battery, which could lead to a better fuel economy for HEVs compared to conventional vehicles. Many EMSs have been proposed by previous

researches. According to the method of algorithm implementation, EMSs are generally divided into two different categories: rule-based EMS and optimization-based EMS [2], [3]. Rule-based EMSs, including deterministic strategies [4]–[6] and fuzzy logic strategies [7]–[9], have been widely adopted in the HEV industry owing to their simplicity and capacity to carry out in real time. For example, Peng et al. presented an improved rule-based energy management algorithm by employing the dynamic programming (DP) which chooses the best actions for the engine in HEVs [5]. Montazeri et al. developed a multi-input fuzzy logic controller to improve the fuel economy for a power-split HEV and yielded reduced fuel consumption compared to conventional rule-based controller [8]. Denis et al. proposed a fuzzy logic-based blended energy management strategy fed with driving condition information and demonstrated the efficiency by simulations [9]. However, these strategies are developed based on the

The associate editor coordinating the review of this manuscript and approving it for publication was Ailong Wu.

engineering experience and specific driving cycles, which makes it difficult to obtain near-optimal control outcome.

For the optimization-based EMS, it mainly focuses on the optimization of the powertrain control in order to achieve optimum performance. Considering the degree of optimization, global optimization-based EMS and online optimization-based EMS are the two main algorithms. DP [10]–[13] is the most representative global optimization-based EMS. It calculates the global optimum solution among the whole driving cycle range based on Bellman's principle [10]. Although it cannot be applied online due to its heavy computational burden and strong dependence on the prior knowledge of the driving cycle, it works as the benchmark of other energy management strategies. An energy management algorithm for HEV was optimized by DP, giving consideration to energy losses and the efficiency during mode shift. A case study proved its effectiveness [11].

Online optimization-based EMSs divide the global optimization problems into a series of local optimization problems in order to reduce the computational effort. The dispensability of future driving condition makes them work in real time [14]. The most popular techniques among them are PMP and ECMS. Model predictive control (MPC) [15], [16] and machine learning (ML) [17]–[19] also gradually attract more attention and are applied to more researches in real-time energy management today. PMP minimizes a Hamiltonian function instantaneously throughout the driving cycle [20]–[22]. Stocker et al. utilized PMP to solve local optimization problems generated from a global optimal control problem, to minimize CO<sub>2</sub> emissions produced by vehicles [22]. MPC enables to work out the power-split ratio over the prediction horizon. Furthermore, in some specific driving conditions, with proper prediction settings, it is possible to achieve the fuel economy similar to DP by MPC-based EMS [15]. ML, one of the core technologies in artificial intelligence (AI) field, is a novel method emerged in EMS in recent years. Liu et al. proposed a reinforcement learning-based EMS for a hybrid electric tracked vehicle [17]. Wu et al. employed Q learning, a famous ML algorithm, to their EMS for a hybrid electric bus. Results demonstrated the achievement in fuel economy under unknown driving condition by comparing with DP-based strategy [18].

ECMS is a more practical approach to implement online as it solves instantaneous minimization problems about cost index, which is represented as the cost function weighted by equivalent factors (EF). ECMS converts electricity consumption to equivalent fuel consumption calculated by EF, and the objective is to minimize the equivalent fuel consumption in every step [23]. Since ECMS shows its sensitivity to EF and fixed EF is unable to adapt to complex real driving conditions, many researchers have proposed adaptive ECMS (A-ECMS) based on the tuning of EF. According to the form of adjustment algorithm, the A-ECMS could be basically divided into three categories: the driving conditions prediction-based A-ECMS, the driving pattern recognition-based A-ECMS and the SOC-based A-ECMS. The concept of

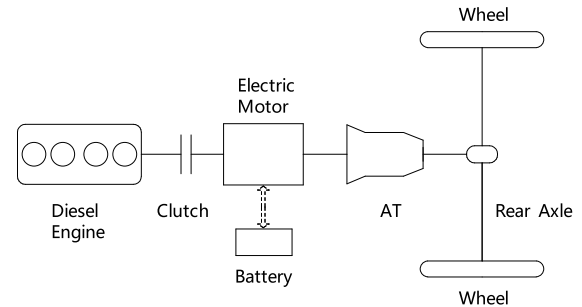


FIGURE 1. Structure of the parallel HEV.

A-ECMS was first proposed by Musardo, and the EF adjustment algorithm is based on driving condition prediction [24]. Zhang et al. used chaining neural network to introduce a new velocity forecasting method, which was subsequently adopted for EF adaptation [25]. For the driving pattern recognition-based A-ECMS [26], [27], a number of typical driving patterns are derived from numerous historical driving data, and then the optimal EF for each typical driving pattern is calculated. During the actual driving conditions, the EF is adjusted along with the typical driving pattern being periodically recognized by the past driving data. SOC-based A-ECMS tunes the EF according to the deviation between actual SOC and reference SOC, to keep SOC near the reference value [28], [29]. However, the previous EF adaptation approaches based on SOC feedback show weak robustness to sustain SOC under different driving conditions.

The main contribution of this paper is that a novel A-ECMS combined with fuzzy logic control, called Fuzzy A-ECMS, is presented to implement real-time energy management. It utilizes a new approach to tune the EF with the fuzzy logic controller, leading to a better SOC trajectory and stronger robustness as well as better fuel economy. The proposed Fuzzy A-ECMS is applied to a parallel HEV and is verified by the comparison with rule-based EMS, conventional SOC-based A-ECMS and standard ECMS under the driving cycle of the Worldwide Harmonized Light Vehicles Test Procedure (WLTC) and the New European Driving Cycle (NEDC) as well as a real driving cycle called Beihang Campus Shuttle Bus Driving Cycle (BCSBDC) with two different initial EF settings.

The remainders of this paper are organized as follows. Section II establishes a parallel HEV model with detailed information about the main components. Section III gives the implementation of the proposed Fuzzy A-ECMS as the real-time energy management strategy for parallel HEV. Then, the simulation is presented and the comparison results are analyzed in section IV. Finally, section V illustrates the conclusions.

## II. HEV MODELING

In this section, the parallel hybrid powertrain configuration of the target HEV is displayed in Fig. 1, where the engine, electric motor (EM), clutch, transmission and battery can be

TABLE 1. Vehicle parameters.

Parameters	Value
Vehicle curb mass (kg)	4500
Static rolling radius of tire (m)	0.414
Dynamic rolling radius of tire (m)	0.44
Frontal area(m <sup>2</sup> )	4.24
Aerodynamic drag coefficient	0.65
Rolling resistance coefficient	0.75
Correction coefficient of rotating mass	1.04

TABLE 2. Engine parameters.

Parameters	Value
Engine displacement (L)	4.5
Number of cylinders	4
Number of strokes	4
Maximum torque (Nm)	770
Maximum rotational speed (rpm)	2500

TABLE 3. Electric motor parameters.

Parameters	Value
Rated power (kW)	80
Maximum power (kW)	133
Maximum torque (Nm)	793
Maximum rotational speed (rpm)	3250

TABLE 4. Gear ratio of transmissions.

Transmission	Gear	Gear ratio
Automatic Transmission	1st	3.1
	2nd	1.81
	3rd	1.41
	4th	1.0
	5th	0.71
Final Drive	1st	1
	2nd	2
Wheel Reducer	1st	1.93

seen intuitively. The engine is a 4.5L four-cylinder diesel engine. The EM can work as both motor and generator, which makes mode switching more flexible. A dry clutch, in order to realize power splitting, is equipped between the engine and the EM, to determine which power is engaged. In the studied configuration, the AMT is located on the main drive shaft, providing a gear reduction to both the engine and the EM, which implies where the torque coupling occurs. According to the proposed powertrain configuration, five different working modes can be applied, which are: EM driving mode, engine driving mode, hybrid driving mode, driving charge mode and regenerative braking mode. Energy management strategies determine the torque split between the engine and the EM as the working mode switches, to realize better fuel economy. The basic parameters of the examined HEV are listed in Table 1 to Table 5.

A. ENGINE MODEL

In this paper, the complex engine system is simplified to a static model based on experimental data and dynamic functions, since the research focus is not the dynamic characteristics of the engine. The engine fuel consumption

TABLE 5. Battery parameters.

Parameters	Value
Number of cells	504
Nominal charge capacity of cell (Ah)	20
Nominal voltage of cell (V)	3.7

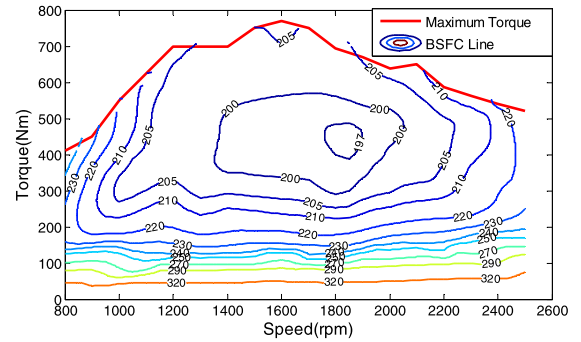


FIGURE 2. Engine fuel consumption contour map.

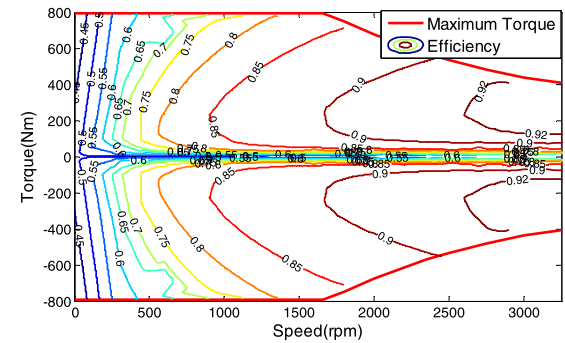


FIGURE 3. EM efficiency map.

contour map is shown in Fig. 2. The transient engine fuel consumption rate can be demonstrated by (1), a function of engine speed and torque. The engine torque is determined by (2).

$$\dot{m}_f(t) = f(T_e(t), n_e(t)) \tag{1}$$

$$T_e = p_e \cdot V_h \cdot i^{-1} \cdot \pi^{-1} \tag{2}$$

where  $\dot{m}_f(t)$  is the engine fuel consumption rate,  $T_e(t)$  is the engine torque,  $n_e(t)$  is the engine rotational speed,  $p_e$  is the effective piston pressure,  $V_h$  is the engine displacement and  $i$  is the strokes.

B. ELECTRIC MOTOR MODEL

The static EM model, based on the EM efficiency contour map (Fig. 3), is of great importance to the energy management strategies. The power consumption of EM can be expressed as a function of EM torque, rotational speed and efficiency, which is formulated in (3) and (4), for motor and generator use respectively.

$$P_{em}(t) = \frac{T_{em}(t) \cdot n_{em}(t)}{9550 \eta_m(t)} \tag{3}$$

$$p_{em}(t) = \frac{T_{em}(t) \cdot n_{em}(t) \cdot \eta_g(t)}{9550} \tag{4}$$

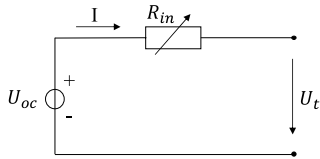


FIGURE 4. The equivalent electrical circuit of the battery.

where  $P_{em}(t)$  is the EM power,  $T_{em}(t)$  is the output torque of EM,  $n_{em}(t)$  is the EM rotational speed,  $\eta_m(t)$  and  $\eta_g(t)$  are the EM efficiency at the current speed and torque when EM operates as a motor and a generator respectively, which can be obtained by look-up table.

### C. BATTERY MODEL

It is difficult to build a precise model of the power battery due to the influence of temperature, voltage, resistance, SOC, etc. In this paper, the Rint model, a widely applied internal resistance model, is adopted to simplify the battery model [30]. The equivalent electrical circuit is shown in Fig. 4. The power equation of the battery can be described in (5).

$$P_{bat}(t) = P_b(t) + R_{in}(t) \cdot I(t)^2 \quad (5)$$

$$U_{oc}(t) = U_t(t) + R_{in}(t) \cdot I(t) \quad (6)$$

where  $P_{bat}(t)$  is the internal battery power,  $P_b(t)$  is the output power of the battery,  $I$  is the current,  $R_{in}$  is the equivalent internal resistance,  $U_{oc}$  is the open-circuit voltage,  $U_t(t)$  is the terminal voltage.

In the battery, SOC is a significant indicator of power consumption and can be calculated by (7) based on Kirchhoff's voltage law.

$$SOC(t) = -\frac{U_{oc}(t) - \sqrt{U_{oc}(t)^2 - 4P_b(t) \cdot R_{in}(t)}}{2Q_{max} \cdot R_{in}(t)} \quad (7)$$

where  $Q_{max}$  is the nominal battery charging capacity.

### D. TRANSMISSION MODEL

The studied HEV is equipped with a fifth-gear automatic transmission, which is closely linked to the fuel economy and driving comfort [31], [32]. Here, neglecting the torsional and lateral vibration, the output torque and wheel rotational speed are formulated as:

$$T_{out}(t) = T_{in}(t) \cdot \eta_t \cdot i_t \cdot i_f \quad (8)$$

$$n_w = \frac{n_e}{i_t \cdot i_f} \quad (9)$$

where  $T_{out}(t)$  and  $T_{in}(t)$  are the output torque and input torque of the transmission, respectively,  $\eta_t$  is the transmission efficiency,  $i_t$  and  $i_f$  are the gear ratio of the transmission and final drive, respectively,  $n_w$  is the wheel rotational speed.

### E. VEHICLE LONGITUDINAL DYNAMIC MODEL

Since fuel economy is the main focus for energy management in this paper, only the longitudinal dynamics of the studied

HEV are considered, ignoring the lateral dynamics, steering dynamics, etc. Therefore, firstly, the equation between the applied torque acting on wheels and the output torque of the engine, EM and brakes can be written as:

$$T_w = \eta_t \cdot i_t \cdot i_f (T_e + T_{em}) + T_b \quad (10)$$

where  $T_w$ ,  $T_e$ ,  $T_{em}$ ,  $T_b$ , are the applied torque acting on wheels, engine torque, EM torque and braking torque, respectively.  $T_w$  can also be derived from (11) according to the longitudinal dynamics, assuming the HEV runs on a horizontal road [33].

$$\begin{cases} T_w = (F_{air} + F_{rolling} + F_{inertia}) \cdot r \\ F_{air} = \frac{1}{2} C_D \rho_d A v^2 \\ F_{rolling} = mg f_r \\ F_{inertia} = \delta m \frac{dv}{dt} \end{cases} \quad (11)$$

where  $F_{air}$ ,  $F_{rolling}$ ,  $F_{inertia}$  are the air resistance, the rolling resistance and the acceleration resistance, respectively.  $C_D$  is the aerodynamic drag coefficient,  $\rho_d$  is the air density,  $A$  is the frontal area,  $v$  is the vehicle velocity,  $m$  is the vehicle mass,  $f_r$  is the rolling resistance coefficient and  $\delta$  is the correction coefficient of rotating mass.

### F. DRIVER MODEL

To better implement the simulation of the studied EMS, a driver model, that determines acceleration and deceleration during driving, is formulated by the proportional-integral (PI) controller [34], as shown in (12) and (13).

$$\alpha(t) = K_p \cdot \Delta v(t) + K_i \int \Delta v(t) dt \quad (12)$$

$$\Delta v(t) = v_{desired} - v_{actual} \quad (13)$$

where  $\alpha(t)$  is the opening of the pedal, with a positive value representing acceleration and a negative value representing braking,  $K_p$  and  $K_i$  are the proportional and integral coefficient, respectively,  $v_{desired}$  is the current target velocity,  $v_{actual}$  is the actual velocity.

### G. PHYSICAL MODEL

In order to obtain simulation results close to real driving condition, in this paper, a physical model with high fidelity is established in the AVL CRUISE software, which is known as an authentic vehicle simulation platform. The final HEV model is shown in Fig. 5.

## III. FUZZY ADAPTIVE-EQUIVALENT CONSUMPTION MINIMIZATION STRATEGY

### A. ENERGY MANAGEMENT PROBLEM FORMULATION

Energy management problems are regarded as optimal control problems, of which the focus is the optimal power distribution between the engine and EM, getting the minimum value of cost function and achieving the best fuel economy, with the satisfaction of a number of constraints. The cost

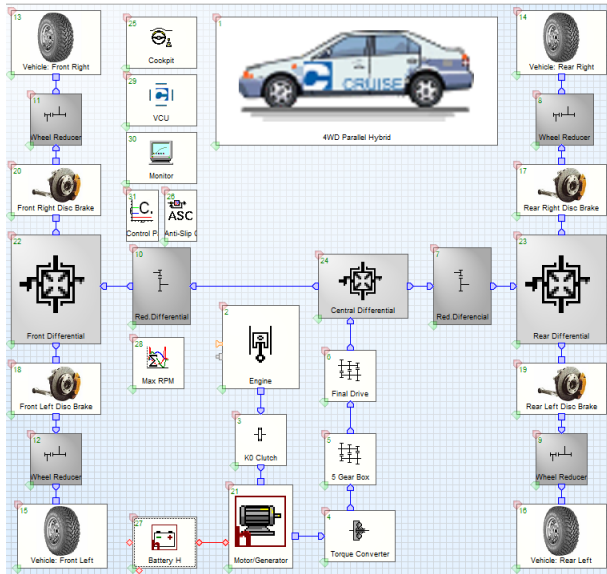


FIGURE 5. Physical model of the parallel HEV.

function  $J_e$  of energy management problems is formulated as:

$$J_e = \int_{t_0}^{t_f} \dot{m}_f(T_e(t), t) dt + f(SOC(t_f)) \quad (14)$$

where  $t_0$  and  $t_f$  are the start and end time of the driving cycle, respectively,  $\dot{m}_f(T_e(t), t)$  is the actual engine fuel consumption rate and  $f(SOC(t_f))$  is a penalty function related to the final SOC.

Taking the actual operating characteristics of HEVs into consideration, the control variables and state variables of the optimal control problems should satisfy the following constraints.

$$\begin{cases} T_{e\_min}(n_e(t)) \leq T_e(t) \leq T_{e\_max}(n_e(t)) \\ n_{e\_min} \leq n_e(t) \leq n_{e\_max} \\ T_{em\_min}(n_{em}(t)) \leq T_{em}(t) \leq T_{em\_max}(n_{em}(t)) \\ n_{em\_min} \leq n_{em}(t) \leq n_{em\_max} \\ SOC_l \leq SOC(t) \leq SOC_h \end{cases} \quad (15)$$

where  $T_{e\_min}(n_e(t))$  and  $T_{e\_max}(n_e(t))$  are the lower and upper engine torque limits at current speed, respectively,  $n_{e\_min}$  is the lower engine speed limit,  $n_{e\_max}$  is the upper engine speed limit,  $T_{em\_min}(n_{em}(t))$  and  $T_{em\_max}(n_{em}(t))$  are the lower and upper EM torque limits at current speed, respectively,  $n_{em\_min}$  is the lower EM speed limit,  $n_{em\_max}$  is the upper EM speed limit,  $SOC_l$  and  $SOC_h$  are the lower and upper battery SOC limits, respectively.

### B. EQUIVALENT CONSUMPTION MINIMIZATION STRATEGY

This paper presents a Fuzzy A-ECMS for real-time energy management, which is developed based on a local optimization control strategy, ECMS, an algorithm derived from Pontryagin's minimum principle (PMP), aiming to minimize

the instantaneous equivalent fuel consumption. According to PMP, the optimal control decision  $u^*(t)$  meeting the minimization of the given Hamiltonian function  $H(x^*(t), u^*(t), \lambda^*(t), t)$  is one of the necessary conditions to get the minimum value of the cost function related to energy management problems [35]. The Hamiltonian function is given by (16), which can be expressed as the sum of actual fuel consumption of the engine and the engine consumption converted from electricity cost.

$$H(SOC(t), T_e(t), \lambda(t), t) = \dot{m}_f(T_e(t), t) + \lambda(t)SOC\dot{(t)} \quad (16)$$

where  $\lambda(t)$  is the co-state variable, which can be calculated as (17) by the co-state dynamics.

$$\dot{\lambda}(t) = \frac{\partial H(SOC(t), T_e(t), \lambda(t), t)}{\partial SOC} = -\lambda(t) \frac{\partial SOC\dot{(t)}}{\partial SOC} \quad (17)$$

The SOC dynamics can be written as:

$$SOC\dot{(t)} = -\frac{I}{Q_{max}} = -\frac{I \cdot U_{oc}}{Q_{max} \cdot U_{oc}} = -\frac{P_{bat}(t)}{3.6E_{bat}(t)} \quad (18)$$

where  $E_{bat}(t)$  is the battery energy. Substituting (18) into (16), the Hamiltonian function is rewritten as:

$$\begin{cases} H(SOC(t), T_e(t), \lambda(t), t) \\ = \dot{m}_f(u(t), t) \\ + \lambda(t) \cdot \left( -\frac{P_{bat}(t) \cdot H_{lhv}}{3.6E_{bat}(t) \cdot H_{lhv}} \right) \\ = \dot{m}_f(u(t), t) + S(t) \cdot \frac{P_{bat}(t)}{H_{lhv}} \\ S(t) = \left( -\frac{H_{lhv}}{3.6E_{bat}(t)} \right) \cdot \lambda(t) \end{cases} \quad (19)$$

where  $H_{lhv}$  is the lower heating value of the fuel,  $S(t)$  represents the EF of the ECMS.

In order to maintain battery performance and extend battery life, SOC change is restricted to a small range, which implies that the open-circuit voltage and internal resistance remain basically unchanged. Consequently,  $\dot{\lambda}(t)$  can be considered as  $\dot{\lambda}(t) = 0$ . Therefore,  $\lambda(t)$  remains constant along the optimal SOC trajectory. Meanwhile, the optimal EF ( $S(t)$ ) could be obtained if the optimal co-state  $\lambda(t)$  is known.

This paper associates EF with SOC deviation from the reference SOC for the sake of battery charge sustainability [25], [36]. The value of EF could be approximated by (20) [37], [38].

$$S(t) = \frac{\eta_{em}}{\eta_e} + 2\delta \frac{H_{lhv}}{E_{bat}(t)} \Delta SOC(t) \quad (20)$$

where  $\eta_{em}$  is the EM efficiency,  $\eta_e$  is the engine efficiency,  $\delta$  is the penalty factor and  $\Delta SOC(t) = SOC_r - SOC(t)$ ,  $\Delta SOC(t)$  is the deviation between the reference SOC ( $SOC_r$ ) and actual SOC ( $SOC(t)$ ).

When the value of EF is determined, the optimal torque distribution can be obtained by (21).

$$[T_{e\_opt}, T_{em\_opt}] = \arg \min \{H(SOC(t), S(t), t)\} \quad (21)$$

where  $T_{e\_opt}$  and  $T_{em\_opt}$  are the optimal torque of engine and EM, respectively.

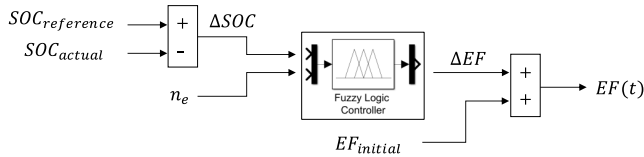


FIGURE 6. Fuzzy logic rule system.

**C. EF ADJUSTMENT ALGORITHM**

The value of EF, determining the power split ratio between the engine and the EM, is crucial to the optimization results of ECMS. This paper uses the iterative method to calculate the approximate optimal EF [39]. The prior knowledge of driving conditions is necessary for the calculation and two standard driving cycles are used for simulation.

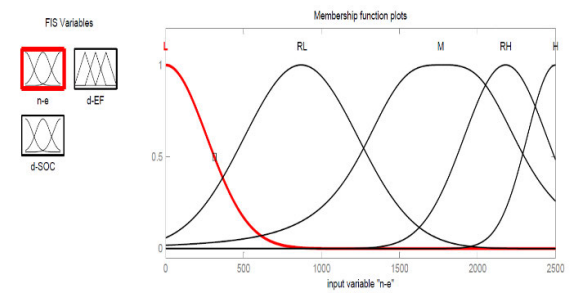
With the optimal constant EF, an approximate global optimal result can be obtained, based on the prior knowledge of the driving cycle. However, in real-world conditions, it is not feasible to get the optimum control with a constant EF, due to the unpredictability of the driving conditions. In the previous researches, an adaptation law, which could be described in (22), was adopted to adjust the EF, leading to an improved fuel economy compared to constant EF.

$$S(k + 1) = S(k) + k_p(SOC_r - SOC(t)) \quad (22)$$

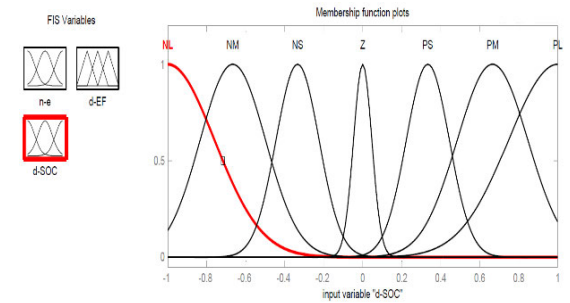
where  $S(k+1)$  presents the new value of EF in the next iteration,  $S(k)$  is the current EF,  $k_p$  is the proportional gain of the feedback controller.

Furthermore, researchers use the PI controller to improve the convergence of EF based on the aforementioned adaptation law. However, the unsatisfactory SOC charge sustainability is still a problem to the real-time control of HEV, which means a significant deviation between the actual SOC and the reference SOC still exists. Therefore, the EF adaptation law with stronger robustness based on SOC deviation is necessary to be employed to balance the battery SOC and enhance robustness. In view of this, considering the strong robustness of fuzzy controller, a new adjustment algorithm with fuzzy logic controller modifying EF as well as sustaining SOC is developed.

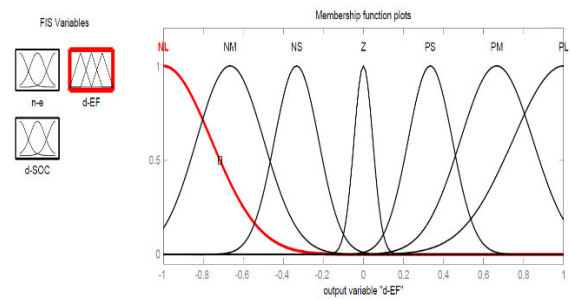
The fuzzy rule system shown in Fig. 6 is applied to calculate the EF adjustment based on the identification of current speed and SOC deviation. There are two inputs and one output of the proposed fuzzy logic controller. One input is  $\Delta SOC$ , the SOC deviation between the actual SOC and reference SOC, defined by seven membership functions (Positive Large, Positive Medium, Positive Small, Zero, Negative Small, Negative Medium and Negative Large). The other one is the current rotational speed of the engine, defined by five membership functions (High, Relatively High, Medium, Relatively Low and Low). The output is the EF adjustment based on the initial EF, which is defined by seven membership functions as  $\Delta SOC$ . According to the characteristics of the EF, more fuel energy will be consumed by increasing the value of EF, resulting in the growth of battery SOC. Conversely, more battery power will be consumed with a drop



(a) Membership function for engine speed



(b) Membership function for ΔSOC



(c) Membership function for EF adjustment

FIGURE 7. Membership functions for inputs and output.

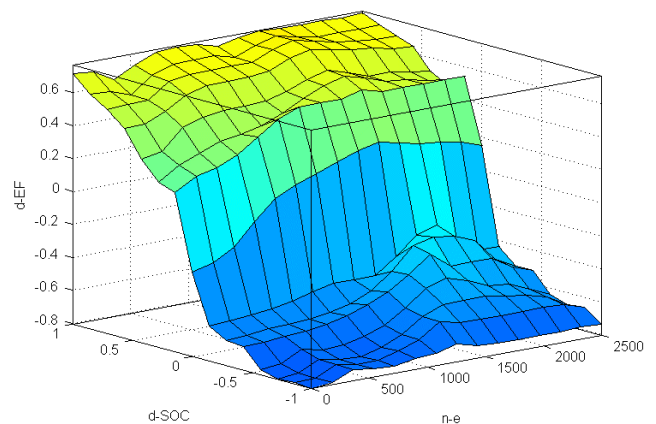


FIGURE 8. Output surface for the fuzzy inference system.

of SOC if the value of EF is reduced. And in the light of engine fuel consumption contour map, the engine works more efficiently in the mid-speed range, while less efficiently in the low-speed range and high-speed range. Consequently, the

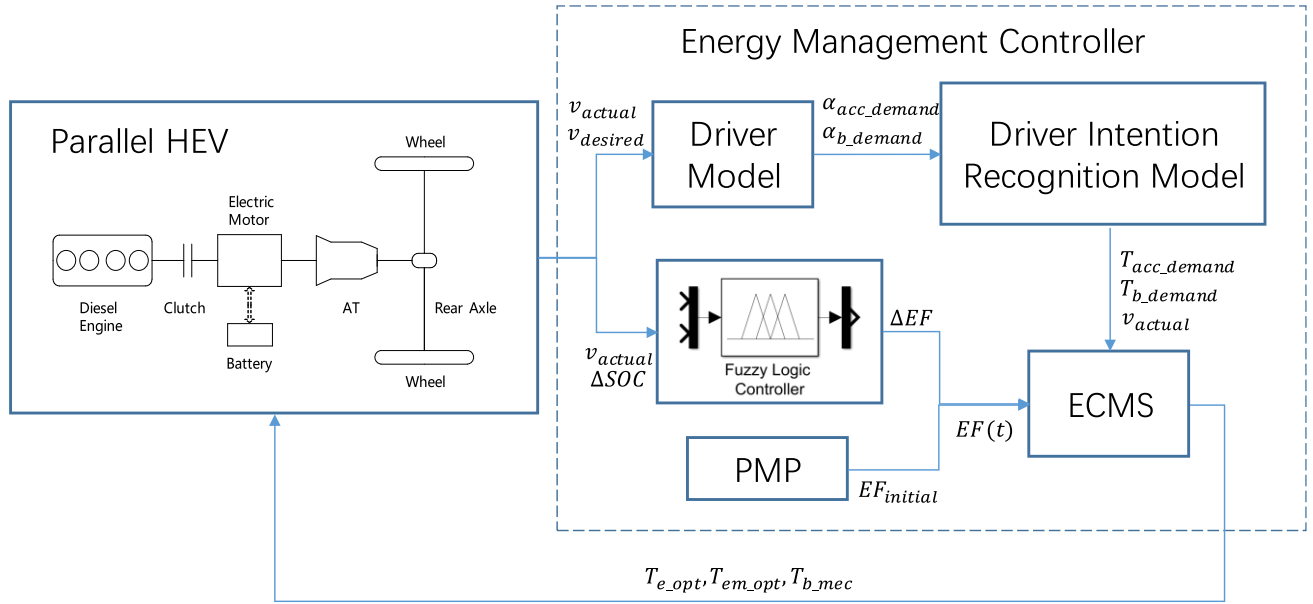


FIGURE 9. The framework of the Fuzzy A-ECMS for a parallel HEV.

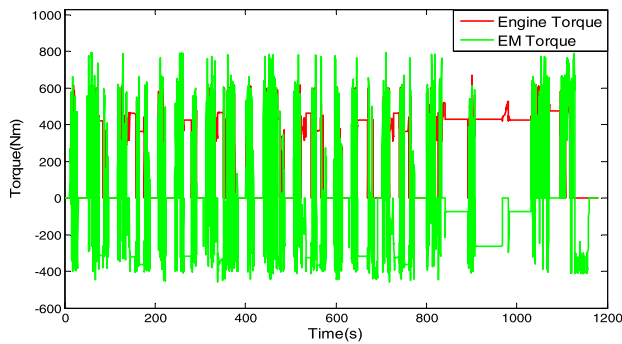


FIGURE 10. Torque distribution in NEDC.

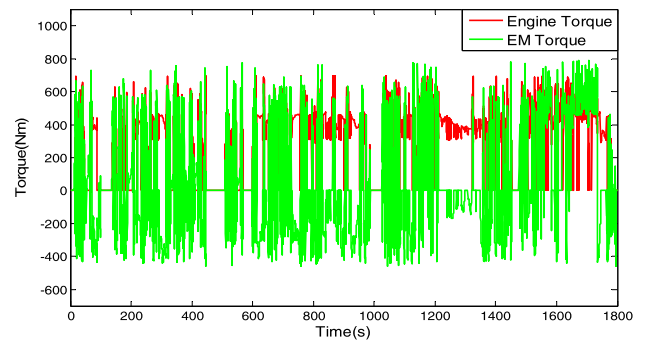


FIGURE 11. Torque distribution in WLTC.

TABLE 6. The fuzzy rules.

$\Delta SOC$		$n_c$						
		NL	NM	NS	Z	PS	PM	PL
L	NL	NL	NM	NS	Z	PS	PM	PL
RL	NL	NL	NM	Z	PS	PM	PL	PL
M	NL	NS	Z	PS	PM	PL	PL	PL
RH	NL	NM	NS	Z	PS	PM	PL	PL
H	NL	NL	NM	Z	PS	PM	PL	PL

fuzzy logic rules are formulated based on relevant heuristic knowledge [40]. The basic control algorithm is that the engine works in the high-efficiency range as much as possible. Additionally, the engine provides additional power to recharge the battery when the SOC reaches its lower threshold. Furthermore, priority is given to motor drive when the vehicle is starting or at low speed.

The membership functions for inputs and output are shown in Fig. 7. Fig. 8 presents the output surface for the fuzzy inference system. The fuzzy rules between output and inputs are formulated in Table 6.

#### D. REAL-TIME ENERGY MANAGEMENT STRATEGY IMPLEMENTATION

Based on the aforementioned ECMS and EF adjustment algorithm, the Fuzzy A-ECMS, of which the framework is presented in Fig. 9, is developed to implement real-time energy management for the parallel HEV.

The vehicle speed information is transferred from the HEV physical model to the driver model, and then the acceleration or brake pedal signal can be obtained. A driver intention recognition module as described in (23) is utilized to identify the overall torque demand of the transmission input axle according to pedal signal and the current speed deviation from target speed.

$$T_{acc\_dem} = \alpha_{acc\_pedal} \cdot (T_{e\_max}(n_e(t)) + T_{em\_max}(n_{em}(t))) \quad (23)$$

where  $T_{acc\_dem}$  is the demand torque on the transmission input axle,  $\alpha_{acc\_pedal}$  is the opening of the acceleration pedal and  $T_{e\_max}(n_e(t))$  and  $T_{em\_max}(n_{em}(t))$  are the maximum torque

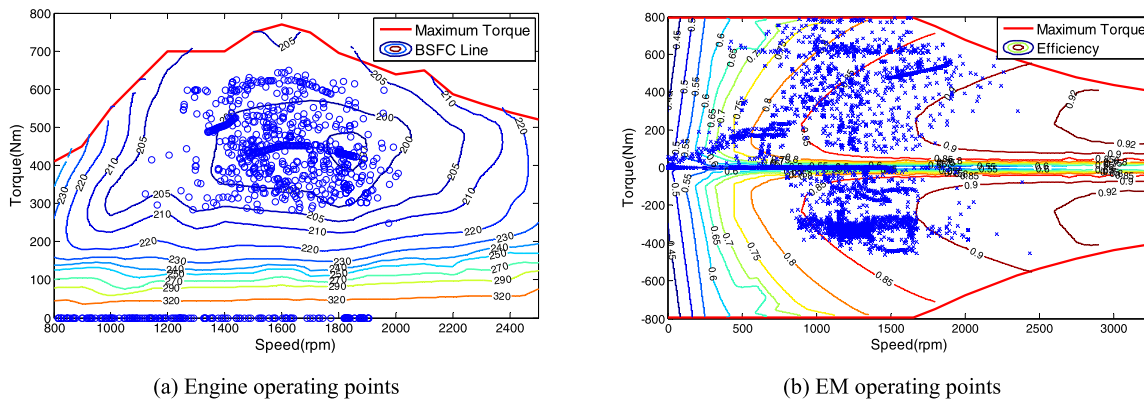


FIGURE 12. Operating points of engine and EM in NEDC.

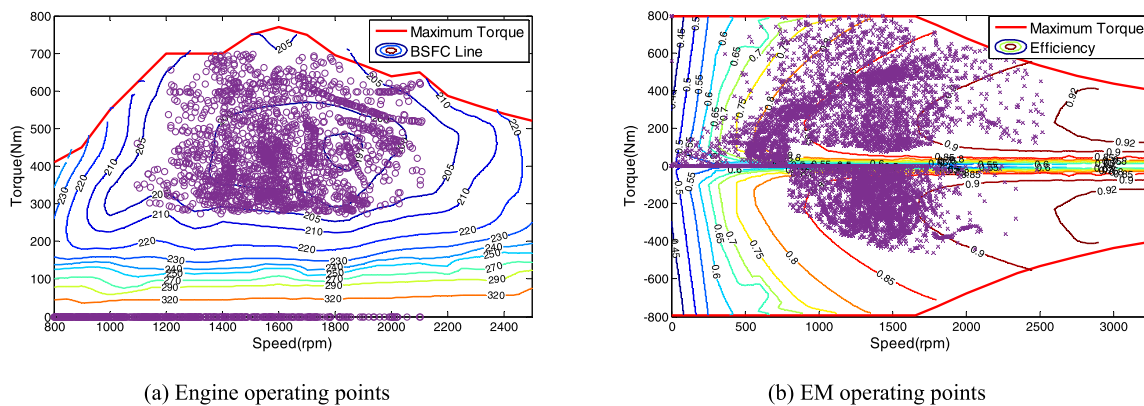


FIGURE 13. Operating points of engine and EM in WLTC.

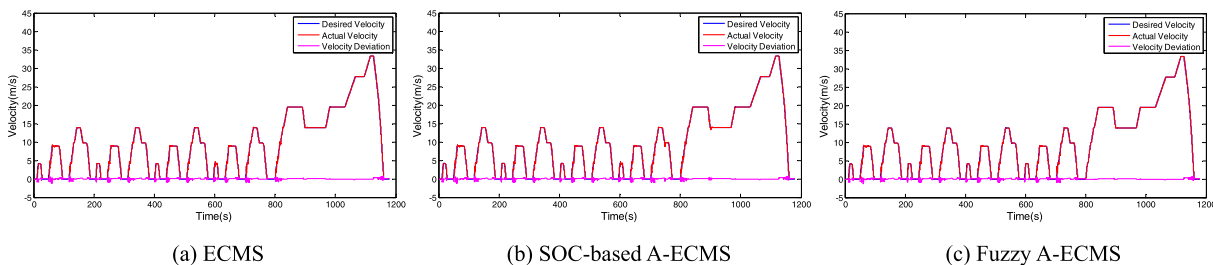


FIGURE 14. Driving cycle tracking in NEDC.

of the engine and the EM at the current rotational speed, respectively.

Then, the proposed Fuzzy A-ECMS determines the instantaneous optimal torque split ratio based on the speed and demand torque information, with the adjustment of EF, which is the sum of the initial near optimal EF calculated by PMP and the output of the fuzzy logic controller.

For the battery charge sustainability, a practical regenerative braking method is used to balance the brake torque split to EM and mechanical brake. The EM works on regenerative braking mode while the brake pedal is depressed, and the torque split to it and mechanical brakes are given by (27).

$$T_{b\_dem} = \alpha_{b\_pedal} \cdot T_{b\_max} \quad (24)$$

$$T_{b\_max} = T_{b\_mec\_max} + T_{em\_max}(n_{em}(t)) \cdot \eta_t \cdot i_t \cdot i_f \quad (25)$$

$$\xi = T_{b\_dem} - T_{em\_max}(n_{em}(t)) \cdot \eta_t \cdot i_t \cdot i_f \quad (26)$$

$$\begin{cases} T_{em\_reg}(t) = T_{em\_max}(n_{em}(t)) & T_{b\_mec}(t) = \xi, \text{ if } \xi > 0 \\ T_{em\_reg}(t) = \frac{T_{b\_dem}}{\eta_t \cdot i_t \cdot i_f} & T_{b\_mec}(t) = 0, \text{ if } \xi \leq 0 \end{cases} \quad (27)$$

where  $T_{b\_dem}$  is the demand brake torque,  $\alpha_{b\_pedal}$  is the opening of brake pedal,  $T_{b\_max}$  is the maximum overall brake torque acting on wheels,  $T_{em\_max}(n_{em}(t))$  is the maximum torque of EM at the current rotational speed,  $T_{em\_reg}(t)$  and  $T_{b\_mec}(t)$  are the torque output from the EM and brake torque acting on wheels from mechanical brakes, respectively.



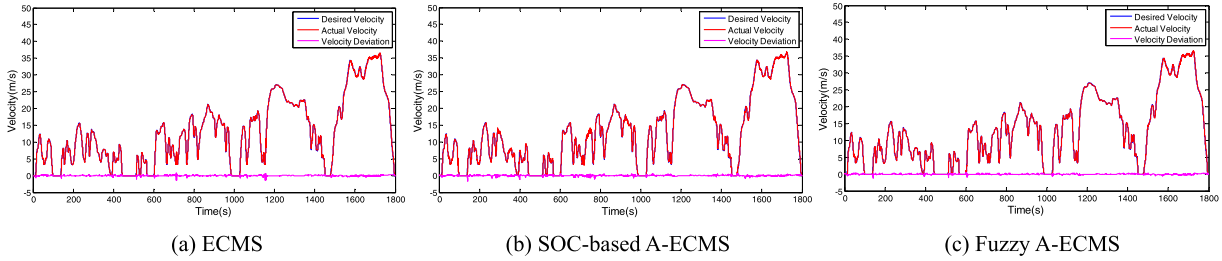


FIGURE 15. Driving cycle tracking in WLTC.

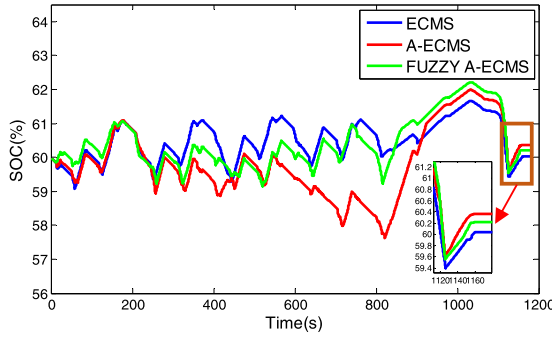


FIGURE 16. Battery SOC trajectory comparison of three EMSs in NEDC.

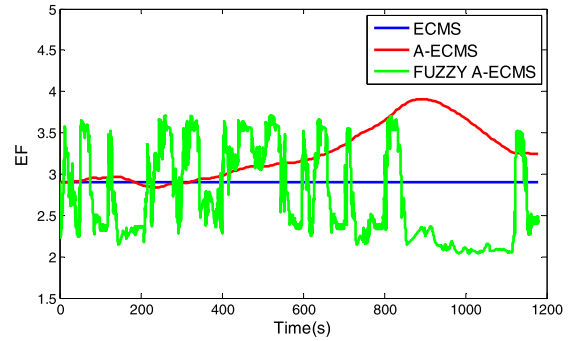


FIGURE 18. EF comparison of three EMSs in NEDC.

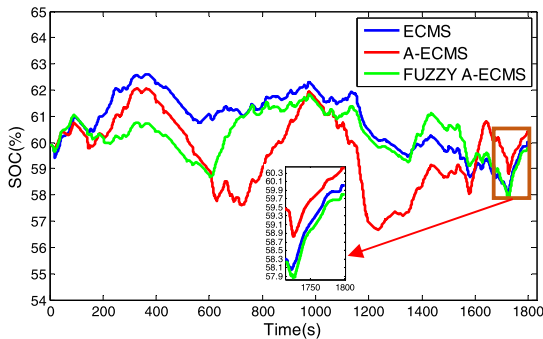


FIGURE 17. Battery SOC trajectory comparison of three EMSs in WLTC.

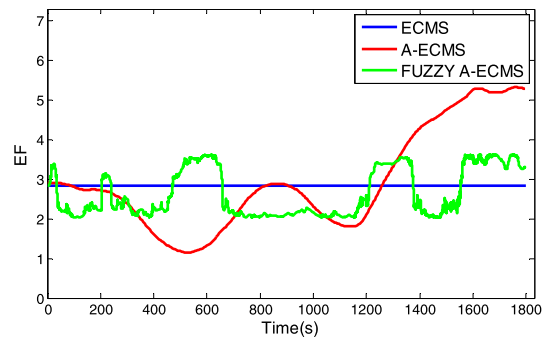


FIGURE 19. EF comparison of three EMSs in WLTC.

IV. SIMULATION VALIDATION AND RESULT ANALYSIS

After establishing the physical model of the parallel HEV in AVL CRUISE software, the real-time energy management controller, Fuzzy A-ECMS, which includes the basic ECMS module and a fuzzy logic controller to regulate the EF based on the SOC deviation, is formulated in MATLAB/Simulink, with the AVL CRUISE interface connecting it to the physical HEV model.

A. COMPARATIVE SIMULATION TEST

To evaluate the optimization performance of the studied control algorithm, simulations under two driving cycles of NEDC and WLTC are carried out. Fig.10. and Fig.11. show the torque distribution between engine and EM in two driving cycles, from which it can be observed that EM works more in starting condition and outputs torque to optimize the engine operating points. The engine works in a relatively

small torque range and charges the battery while SOC is low, which contributes to the fuel economy and SOC sustainability. As we can see from Fig.12. and Fig. 13., which represent operating points of engine and EM under different driving cycles, in the whole simulation period, the engine basically works in low fuel consumption rate areas, with the majority of the brake specific fuel consumption lower than 205 g/kwh, while EM works more frequently and more scattered, with most of the efficiency higher than 0.8. The low engine fuel consumption rate and high EM efficiency guarantee reduction in total fuel consumption of the hybrid powertrain system.

For comparison purpose, the comparative simulation of the Fuzzy A-ECMS and other three real-time controllers, SOC-based A-ECMS, standard ECMS and rule-based EMS, is made under the driving cycles of NEDC and WLTC. To maintain a good performance of the electric power battery, the initial value of SOC is chosen as 0.6. The approximate

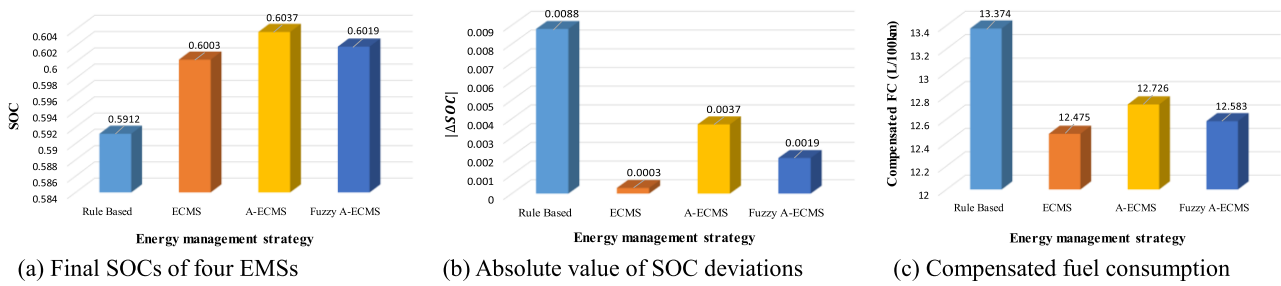


FIGURE 20. Comparison of four EMSs in NEDC.

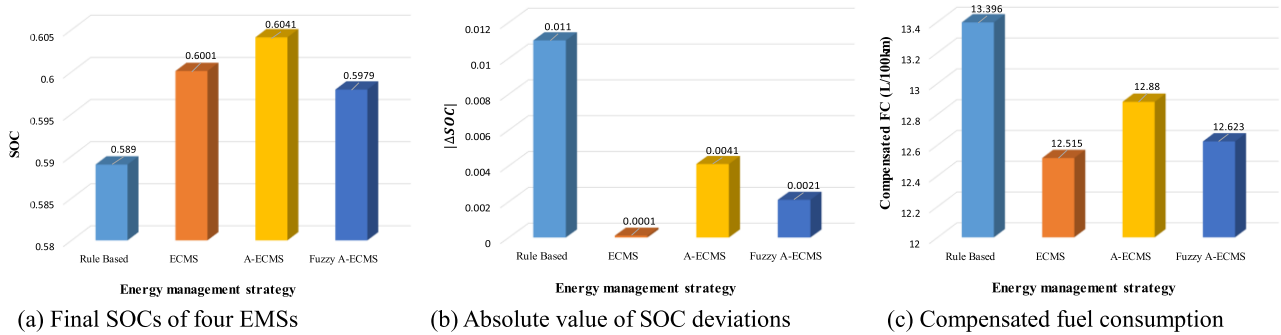


FIGURE 21. Comparison of four EMSs in WLTC.

optimal values of EF for ECMS, which are also determined as the initial EF for Fuzzy A-ECMS and SOC-based A-ECMS, are set as 2.9 and 2.84 in NEDC and WLTC, respectively, using iterative method. In real driving conditions, the initial EF can be selected as  $\eta_{em}/\eta_e$  [38] according to (20).

It can be seen in Fig. 14. and Fig. 15., the actual velocity follows the target velocity well, with maximum velocity deviation of about 1.2 m/s for NEDC and 1.05 m/s for WLTC. Fig. 16. and Fig. 17 show the battery SOC trajectories obtained by the three different EMSs under different driving cycles. In NEDC, the final SOC deviation of Fuzzy A-ECMS is 0.0019, which is slightly larger than the value of ECMS, 0.0003, but smaller than that of SOC-based A-ECMS, 0.0037. The maximum deviation between actual SOC and reference SOC of SOC-based A-ECMS among the entire driving cycle is 0.0259, followed by Fuzzy A-ECMS with the value of 0.0221, while ECMS generates the minimum value, 0.0167. The near optimal SOC trajectory of ECMS is based on the prior knowledge of driving cycle, while Fuzzy A-ECMS presents better performance in SOC charge sustainability, maintaining SOC deviation within a smaller range, compared with SOC-based A-ECMS.

In WLTC, Fuzzy A-ECMS presents a value of 0.0021 for the final SOC deviation, and the value of ECMS and SOC-based A-ECMS are 0.0001 and 0.0041, respectively. The maximum SOC deviation of Fuzzy A-ECMS throughout the driving cycle is 0.0213, which is the smallest value in the meanwhile, followed by that of ECMS and SOC-based A-ECMS, which are 0.0261 and 0.0333, respectively.

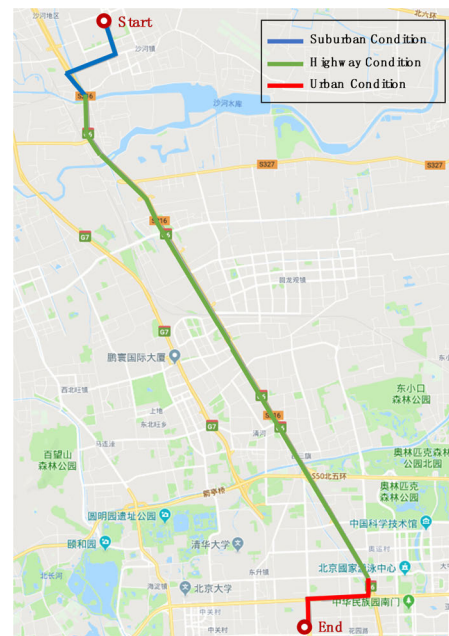


FIGURE 22. GPS route of Beihang campus shuttle bus.

The results substantiate the robustness of Fuzzy A-ECMS compared to conventional SOC-based A-ECMS with a more stable SOC trajectory, verifying the performance in improving SOC charge sustainability.

Fig. 18. and Fig. 19. illustrate the EF adaptation behavior of the three EMSs under two driving cycles. It is clear that the

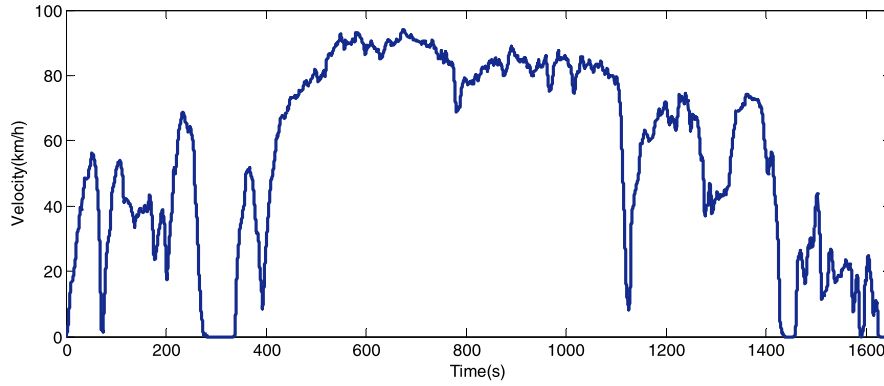


FIGURE 23. Beihang campus shuttle bus driving cycle.

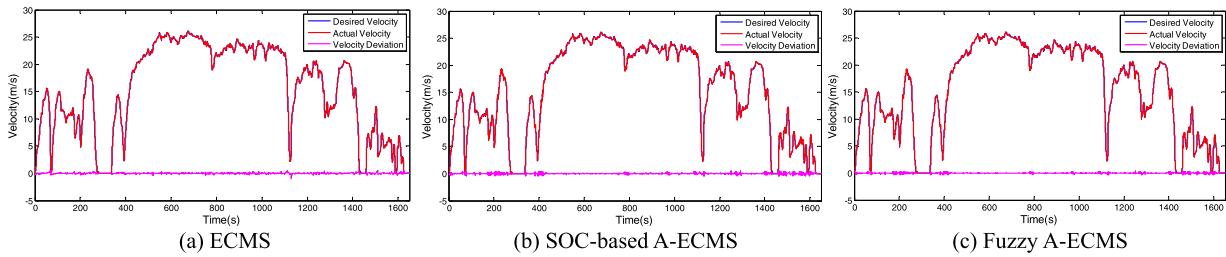


FIGURE 24. Driving cycle tracking in BCSBDC.

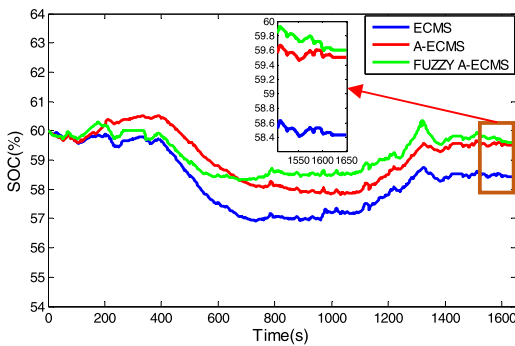


FIGURE 25. Battery SOC trajectory comparison of three EMSs in BCSBDC.

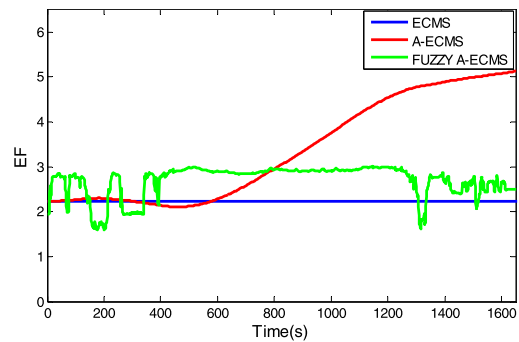


FIGURE 26. EF comparison of three EMSs in BCSBDC.

EF of fuzzy A-ECMS fluctuates more frequently than that of SOC-based A-ECMS. This can be explained by the difference of EF adjustment algorithm – in other words, the EF of Fuzzy A-ECMS is adjusted according to the real-time SOC deviation and engine velocity, while the EF of SOC-based A-ECMS is modified periodically and based on the value of the previous step. For Fuzzy A-ECMS, when the value of SOC is larger than reference SOC, the EF decreases a certain range so that more electricity will be consumed to make SOC closer to reference SOC. Conversely, if SOC is below reference SOC, the EF increases to make more charge behavior. For SOC-based A-ECMS, the EF is tuned after a short period and based on the previous value, which causes a certain lag for the adjustment. According to the EF adjustment performance and data analysis, it can be concluded that the EF adaptation

law of Fuzzy A-ECMS is more robust to adjust EF flexibly and achieves better SOC charge sustainability.

Furthermore, in order to evaluate the fuel economy of the proposed Fuzzy A-ECMS, a comparison with three other EMSs is presented in Fig.20. and Fig. 21. The SOC-compensated fuel consumption is employed to make a fair comparative study. As we can see, in NEDC, the compensated fuel consumptions for Fuzzy A-ECMS, rule-based EMS and SOC-based A-ECMS are 12.583, 13.374 and 12.726, respectively. That is to say, Fuzzy A-ECMS shows 5.91% and 1.12% improvements in fuel economy over rule-based EMS and SOC-based A-ECMS, respectively. In WLTC, for the four EMSs mentioned above, the compensated fuel consumptions are 12.623, 13.396 and 12.88, respectively. The proposed Fuzzy A-ECMS improves fuel economy by 5.77% and 1.20%

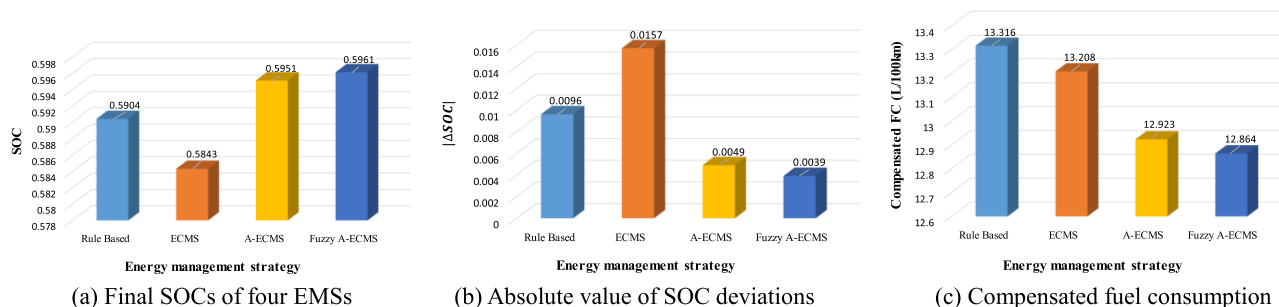


FIGURE 27. Comparison of four EMSs in BCSBDC.

compared with rule-based EMS and SOC-based A-ECMS. In both standard driving cycles, the optimal ECMS works as the benchmark.

### B. SIMULATION TEST UNDER A REAL DRIVING CYCLE

To verify the effectiveness of the proposed EMS under real driving cycles, the driving data on a real road condition is collected and fitted to a driving cycle. The route of Beihang Campus Shuttle Bus is chosen to be the target driving cycle taking into account the typicality of the driving conditions it contains, including typical suburban condition, highway condition and urban condition. Fig. 23 shows the final real driving cycle, namely Beihang Campus Shuttle Bus Driving Cycle (BCSBDC).

To better simulate the actual driving conditions, the initial EF is selected as 2.23 according to (20), in which the  $\eta_{em}$  is 87% and the  $\eta_e$  is 39%. The initial value of SOC is chosen as 0.6.

It can be seen in Fig. 24., the actual velocity follows the target velocity well, with maximum velocity deviation of about 0.86m/s. Fig. 25. shows the battery SOC trajectories obtained by the three different EMSs. The final SOC deviation of Fuzzy A-ECMS is 0.0039, which is slightly smaller than the value of SOC-based A-ECMS, 0.0049, and much smaller than that of ECMS, 0.0157. The maximum deviation between actual SOC and reference SOC of Fuzzy A-ECMS among the entire driving cycle is 0.0169, followed by SOC-based A-ECMS with the value of 0.0218, and ECMS generates the maximum value, 0.031. It is clear that ECMS cannot generate near optimal SOC trajectory when the initial EF is not set based on driving cycles. On the contrary, Fuzzy A-ECMS still presents better performance in SOC charge sustainability, maintaining SOC deviation within a smaller range, compared with SOC-based A-ECMS and ECMS. Fig. 26. illustrates the EF adaptation behavior of the three EMSs under BCSBDC. It shows similar performance as in NEDC and WLTC.

Furthermore, as we can see, in Fig. 27., the compensated fuel consumptions for Fuzzy A-ECMS, rule-based EMS, ECMS and SOC-based A-ECMS are 12.864, 13.316, 13.208 and 12.923, respectively. In other words, Fuzzy A-ECMS shows 3.39%, 2.60% and 0.46% improvements in fuel economy over rule-based EMS, ECMS and SOC-based A-ECMS in real driving conditions, respectively.

### V. CONCLUSION

This article aims to improve the fuel economy and the SOC charge sustainability of the parallel HEV, with the proposal of a novel real-time EMS, namely, Fuzzy A-ECMS. In this study, the ECMS, which is derived from PMP algorithm, is adopted in order to gain approximate optimal fuel economy under real-time driving conditions. For the SOC charge sustainability, an EF adaptation law is developed by utilizing fuzzy logic controller based on SOC deviation. Compared to rule-based EMS and conventional SOC-based A-ECMS, Fuzzy A-ECMS improves the fuel economy from 1.12% to 5.91% under NEDC and WLTC when the initial EFs are set as the optimal EF for ECMS, as well as shows stronger robustness in the SOC charge sustainability. Further, under real driving cycle, the proposed Fuzzy A-ECMS presents 0.46% to 3.39% improvements in fuel economy when the initial EF is not set based on prior knowledge of driving cycle, verifying the feasibility and effectiveness of the proposed Fuzzy A-ECMS under different conditions. In future research, we would like to explore the influence of driver factors and velocity prediction on the performance of energy management strategies.

### ACKNOWLEDGMENT

The authors acknowledge the support of Beijing Key Laboratory for High-efficient Power Transmission and System Control of New Energy Resource Vehicle, the Fundamental Research Funds for the Central Universities and University Institute for Automobile Research (INSIA), Universidad Politécnic de Madrid for HEV modeling.

### REFERENCES

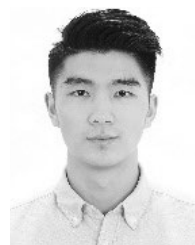
- [1] F. Ji, Y. Bao, Y. Zhou, F. Du, H. Zhu, S. Zhao, G. Li, X. Zhu, and S. Ding, "Investigation on performance and implementation of Tesla turbine in engine waste heat recovery," *Energy Convers. Manage.*, vol. 179, pp. 326–338, Jan. 2019.
- [2] C. M. Martinez, X. Hu, D. Cao, E. Velenis, B. Gao, and M. Wellers, "Energy management in plug-in hybrid electric vehicles: Recent progress and a connected vehicles perspective," *IEEE Trans. Veh. Technol.*, vol. 66, no. 6, pp. 4534–4549, Jun. 2017.
- [3] P. Zhang, F. Yan, and C. Du, "A comprehensive analysis of energy management strategies for hybrid electric vehicles based on bibliometrics," *Renew. Sustain. Energy Rev.*, vol. 48, pp. 88–104, Aug. 2015.
- [4] T. Hofman, R. M. van Druten, A. F. A. Serrarens, and M. Steinbuch, "Rule-based energy management strategies for hybrid vehicles," *Int. J. Electr. Hybrid Veh.*, vol. 1, no. 1, pp. 71–94, 2007.

- [5] J. Peng, H. He, and R. Xiong, "Rule based energy management strategy for a series-parallel plug-in hybrid electric bus optimized by dynamic programming," *Appl. Energy*, vol. 185, pp. 1633–1643, Jan. 2017.
- [6] H. Banvait, S. Anwar, and Y. Chen, "A rule-based energy management strategy for plug-in hybrid electric vehicle (PHEV)," in *Proc. Amer. Control Conf. (ACC)*, Jun. 2009, pp. 3938–3943.
- [7] S. G. Li, S. M. Sharkh, F. C. Walsh, and C. N. Zhang, "Energy and battery management of a plug-in series hybrid electric vehicle using fuzzy logic," *IEEE Trans. Veh. Technol.*, vol. 60, no. 8, pp. 3571–3585, Oct. 2011.
- [8] M. Montazeri-Gh and M. Mahmoodi-K, "Development a new power management strategy for power split hybrid electric vehicles," *Transp. Res. D, Transp. Environ.*, vol. 37, pp. 79–96, Jun. 2015.
- [9] N. Denis, M. R. Dubois, and A. Desrochers, "Fuzzy-based blended control for the energy management of a parallel plug-in hybrid electric vehicle," *IET Intell. Transp. Syst.*, vol. 9, no. 1, pp. 30–37, Feb. 2015.
- [10] Z. Song, H. Hofmann, J. Li, X. Han, and M. Ouyang, "Optimization for a hybrid energy storage system in electric vehicles using dynamic programming approach," *Appl. Energy*, vol. 139, pp. 151–162, Feb. 2015.
- [11] W. Zhuang, X. Zhang, D. Li, L. Wang, and G. Yin, "Mode shift map design and integrated energy management control of a multi-mode hybrid electric vehicle," *Appl. Energy*, vol. 204, pp. 476–488, Oct. 2017.
- [12] L. Li, C. Yang, Y. Zhang, L. Zhang, and J. Song, "Correctional DP-based energy management strategy of plug-in hybrid electric bus for city-bus route," *IEEE Trans. Veh. Technol.*, vol. 64, no. 7, pp. 2792–2803, Jul. 2015.
- [13] Z. Chen, C. C. Mi, J. Xu, X. Gong, and C. You, "Energy management for a power-split plug-in hybrid electric vehicle based on dynamic programming and neural networks," *IEEE Trans. Veh. Technol.*, vol. 63, no. 4, pp. 1567–1580, May 2013.
- [14] W. Enang and C. Bannister, "Modelling and control of hybrid electric vehicles (A comprehensive review)," *Renew. Sustain. Energy Rev.*, vol. 74, pp. 1210–1239, Jul. 2017.
- [15] H. Wang, Y. Huang, A. Khajepour, and Q. Song, "Model predictive control-based energy management strategy for a series hybrid electric tracked vehicle," *Appl. Energy*, vol. 182, pp. 105–114, Nov. 2016.
- [16] S. Xie, X. Hu, Z. Xin, and L. Li, "Time-efficient stochastic model predictive energy management for a plug-in hybrid electric bus with an adaptive reference state-of-charge advisory," *IEEE Trans. Veh. Technol.*, vol. 67, no. 7, pp. 5671–5682, Jul. 2018.
- [17] T. Liu, Y. Zou, D. Liu, and F. Sun, "Reinforcement learning of adaptive energy management with transition probability for a hybrid electric tracked vehicle," *IEEE Trans. Ind. Electron.*, vol. 62, no. 12, pp. 7837–7846, Dec. 2015.
- [18] J. Wu, H. He, J. Peng, Y. Li, and Z. Li, "Continuous reinforcement learning of energy management with deep Q network for a power split hybrid electric bus," *Appl. Energy*, vol. 222, pp. 799–811, Jul. 2018.
- [19] T. Liu, X. Hu, S. E. Li, and D. Cao, "Reinforcement learning optimized look-ahead energy management of a parallel hybrid electric vehicle," *IEEE/ASME Trans. Mechatronics*, vol. 22, no. 4, pp. 1497–1507, Aug. 2017.
- [20] N. Kim, S. Cha, and H. Peng, "Optimal control of hybrid electric vehicles based on Pontryagin's minimum principle," *IEEE Trans. Control Syst. Technol.*, vol. 19, no. 5, pp. 1279–1287, Sep. 2011.
- [21] L. Serrao, S. Onori, and G. Rizzoni, "ECMS as a realization of Pontryagin's minimum principle for HEV control," in *Proc. Amer. Control Conf.*, Jun. 2009, pp. 3964–3969.
- [22] S. Stockar, V. Marano, M. Canova, G. Rizzoni, and L. Guzzella, "Energy-optimal control of plug-in hybrid electric vehicles for real-world driving cycles," *IEEE Trans. Veh. Technol.*, vol. 60, no. 7, pp. 2949–2962, Sep. 2011.
- [23] C. Hou, M. Ouyang, L. Xu, and H. Wang, "Approximate Pontryagin's minimum principle applied to the energy management of plug-in hybrid electric vehicles," *Appl. Energy*, vol. 115, pp. 174–189, Feb. 2014.
- [24] C. Musardo, G. Rizzoni, Y. Guezennec, and B. Staccia, "A-ECMS: An adaptive algorithm for hybrid electric vehicle energy management," *Eur. J. Control*, vol. 11, no. 4, pp. 509–524, 2005.
- [25] F. Zhang, J. Xi, and R. Langari, "Real-time energy management strategy based on velocity forecasts using V2V and V2I communications," *IEEE Trans. Intell. Transp. Syst.*, vol. 18, no. 2, pp. 416–430, Feb. 2017.
- [26] B. Gu and G. Rizzoni, "An adaptive algorithm for hybrid electric vehicle energy management based on driving pattern recognition," in *Proc. ASME Int. Mech. Eng. Congr. Expo.*, Nov. 2006, pp. 249–258.
- [27] Z. Lei, D. Qin, Y. Liu, Z. Peng, and L. Lu, "Dynamic energy management for a novel hybrid electric system based on driving pattern recognition," *Appl. Math. Model.*, vol. 45, pp. 940–954, May 2017.
- [28] A. Chasse, G. Corde, A. D. Mastro, and F. Perez, "Online optimal control of a parallel hybrid with after-treatment constraint integration," in *Proc. IEEE Vehicle Power Propuls. Conf.*, Sep. 2010, pp. 1–6.
- [29] S. Onori, L. Serrao, and G. Rizzoni, "Adaptive equivalent consumption minimization strategy for hybrid electric vehicles," in *Proc. ASME Dyn. Syst. Control Conf.*, Jan. 2010, pp. 499–505.
- [30] P. Shen, Z. Z. Zhao, X. Zhan, and J. Li, "Particle swarm optimization of driving torque demand decision based on fuel economy for plug-in hybrid electric vehicle," *Energy*, vol. 123, pp. 89–107, Mar. 2017.
- [31] P. Dong, Y. Liu, P. Tenberge, and X. Xu, "Design and analysis of a novel multi-speed automatic transmission with four degrees-of-freedom," *Mech. Mach. Theory*, vol. 108, pp. 83–96, Feb. 2017.
- [32] X. Xu, P. Dong, Y. Liu, and H. Zhang, "Progress in automotive transmission technology," *Automot. Innov.*, vol. 1, no. 3, pp. 187–210, Jul. 2018.
- [33] X. Xu, Y. Liang, M. Jordan, P. Tenberge, and P. Dong, "Optimized control of engine start assisted by the disconnect clutch in a P2 hybrid automatic transmission," *Mech. Syst. Signal Process.*, vol. 124, pp. 313–329, Jun. 2019.
- [34] S. Han, F. Zhang, and J. Xi, "A real-time energy management strategy based on energy prediction for parallel hybrid electric vehicles," *IEEE Access*, vol. 6, pp. 70313–70323, 2018.
- [35] R. E. Kalman, P. L. Falb, and M. A. Arbib, *Topics in Mathematical System Theory*. New York, NY, USA: McGraw-Hill, 1969.
- [36] H. Kazemi, Y. P. Fallah, A. Nix, and S. Wayne, "Predictive AECMS by utilization of intelligent transportation systems for hybrid electric vehicle powertrain control," *IEEE Trans. Intell. Veh.*, vol. 2, no. 2, pp. 75–84, Jun. 2017.
- [37] A. Chasse, A. Sciarretta, and J. Chauvin, "Online optimal control of a parallel hybrid with costate adaptation rule," *IFAC Proc. Volumes*, vol. 43, no. 7, pp. 99–104, Jul. 2010.
- [38] S. Yang, W. Wang, F. Zhang, Y. Hu, and J. Xi, "Driving-style-oriented adaptive equivalent consumption minimization strategies for HEVs," *IEEE Trans. Veh. Technol.*, vol. 67, no. 10, pp. 9249–9261, Oct. 2018.
- [39] F. Zhang, H. Liu, Y. Hu, and J. Xi, "A supervisory control algorithm of hybrid electric vehicle based on adaptive equivalent consumption minimization strategy with fuzzy PI," *Energies*, vol. 9, no. 11, p. 919, Nov. 2016.
- [40] S. Wang, Y. Liu, Z. Wang, P. Dong, Y. J. Cheng, X. Xu, and P. Tenberge, "Adaptive fuzzy iterative control strategy for the wet-clutch filling of automatic transmission," *Mech. System Signal Process.*, vol. 130, pp. 164–182, Sep. 2019.



**SHUHAN WANG** received the B.S. degree in mechanical design and manufacturing and automation from the Harbin Institute of Technology, Harbin, China, in 2002, and the Ph.D. degree in vehicle engineering from Beihang University (BUAA), Beijing, China, in 2009.

From 2007 to 2008, he was a Joint Ph.D. Student with the Chemnitz University of Technology, Germany. He is currently an Associate Professor with the School of Transportation Science and Engineering, BUAA, and the Deputy Director of the National Passenger Vehicle Automatic Transmission Engineering Technology Research Center. In 2016, he won the First Prize of the National Science and Technology Progress Award (the third finisher).



**KINGSHUAI HUANG** received the B.S. degree in vehicle engineering from Beihang University (BUAA), Beijing, China, in 2017, where he is currently pursuing the M.S. degree in vehicle engineering.

His research interests include optimal control of hybrid electric vehicles and energy management with artificial intelligence.



**JOSÉ MARÍA LÓPEZ** received the Ph.D. degree in mechanical engineer.

He is currently a Full Professor with the Technical University of Madrid (UPM), Spain, and the Director of the University Institute of Automobile Research Francisco Aparicio Izquierdo (INSIA). He is also the Head of the Alternative Propulsion Systems Unit, INSIA. He is also the Director of the master's degree in automotive engineering and the master's degree in hybrid and electric vehicle engineering of INSIA's and UPM's own titles and a member of the national and international technical committees of the automobile. He has extensive research experience in the field of alternative vehicle propulsion systems (hybrid, electric, and fuel cell) and polluting emissions. His current research interests include the development of models of propulsion systems for hybrid and electric vehicles and their integration and validation in vehicles, as well as the field of polluting emissions and biofuels.



**XIANGYANG XU** received the B.S. and M.S. degrees in vehicle engineering from the Beijing Institute of Technology (BIT), Beijing, China, in 1987 and 1990, respectively, and the Ph.D. degree in mechanical and electronic engineering from the Harbin Institute of Technology, Harbin, China, in 1999.

He is currently a Professor and the Director of the Beijing Key Laboratory for High-efficient Powertrain and System Control of New Energy Resource Vehicle, Beihang University (BUAA). He has developed the world's first front-drive eight-speed automatic transmission (8AT) and its series of products. In 2016, he won the First Prize of the National Science and Technology Progress Award (the first finisher).



**PENG DONG** received the B.S. degree in industrial engineering from Shandong University, Shandong, China, in 2008, the M.S. degree in vehicle engineering from Beihang University (BUAA), Beijing, China, in 2011, and the Ph.D. degree in mechanical engineering from Ruhr Bochum University, Germany, in 2015.

He is currently a Lecturer with the School of Transportation Science and Engineering, BUAA. His research interests include basic theory and scientific application of new energy vehicle power transmission systems, vehicle transmission and control, multigear automatic transmission, and gear fatigue life prediction.

...